Physica A 586 (2022) 126517

Contents lists available at ScienceDirect

Physica A

journal homepage: www.elsevier.com/locate/physa

Resilience assessment of an urban rail transit network: A case study of Chengdu subway

Jinqu Chen [a], Jie Liu [b], Qiyuan Peng [a,c,d], Yong Yin [a,c,d,*]

[a] School of Transportation and Logistics, Southwest Jiaotong University, Chengdu 611756, China
[b] Faculty of Transportation Engineering, Kunming University of Science and Technology, Kunming 650093, China
[c] National United Engineering Laboratory of Integrated and Intelligent Transportation, Chengdu 611756, China
[d] National Engineering Laboratory of Integrated Transportation Big Data Application Technology, Chengdu 611756, China

ARTICLE INFO

Article history:
Received 9 March 2021
Received in revised form 17 September 2021
Available online 12 October 2021

Keywords:
Urban rail transit
Resilience
Effective path betweenness
Modified resilience metric
Resilience triangle

ABSTRACT

Existing studies seldom consider network structure and passenger travel demand jointly, and certain impractical assumptions are generally considered for assessing the resilience of an urban rail transit (URT) network. To address the abovementioned limitations, we have proposed a performance indicator called the demand–impedance (DI) indicator, in which demand and impedance are reflected by passenger trips and travel time. By considering effective travel paths (ETPs) and passengers' path choice behavior, we have proposed a node centrality called effective path betweenness (EPB) by modifying the betweenness centrality (BC) to evaluate the importance of stations. The performance curve of a URT network during the attack and repair processes is depicted using the DI indicator, and a modified resilience metric is formulated by referring to the resilience triangle. The model application in the Chengdu subway network demonstrates that the correlation coefficient between the EPB and BC of stations is 0.901, which indicates that stations with a higher EPB are inclined to have a higher BC. The Chengdu subway network demonstrates a higher resilience under random disturbances than it does under malicious disturbances. Disturbance duration, passengers' tolerance time, and rescue ability on the Chengdu subway network significantly affect its resilience. Several practical suggestions involving the management of disturbances, shortening the emergency response time, providing passenger services, and improving emergency rescue ability are provided for managing the Chengdu subway system under disturbances.

1. Introduction

By the end of 2020, 45 cities started operating an urban rail transit (URT) system in mainland China. The number of operating stations and operating mileage were 4,681 and 7,969.7 km, respectively [1]. The URT system is the backbone of the public transit system in China's metropolises, which has greatly facilitated the daily commute of passengers. However, the URT system in mainland China faces severe challenges caused by the increasingly complex operating environment. For instance, in January 2013, the derailment of a train occurred in the Kunming subway system, which led to a fatality and an injury [2]. In April 2015, a human stampede disturbance at the Huangbeiling station in the Shenzhen subway system resulted in nine non-fatal injuries [3]. In January 2018, trains on the Xi'an subway line 2 were delayed for more than 20 min owing to the failure of the railroad turnouts of the line [4]. In January 2019, equipment failure on Shanghai subway

* Correspondence to: Xipu Campus, Southwest Jiaotong University, West Park of Hi-Tech Zone, Chengdu, Sichuan, 611756, China.
E-mail address: yinyong@home.swjtu.edu.cn (Y. Yin).

https://doi.org/10.1016/j.physa.2021.126517
0378-4371/

Table 1
Studies on assessing a URT network's resilience.

Reference	Network	Performance indicator	Resilience metric
Cox et al. [30]	WN	Changes in the total number of passenger trips	Degree of deviation between the estimated total number of passenger trips reduction and the possible maximum potential reduction
Jin et al. [27]	DN	Amount of satisfied travel demand	Fraction of satisfied travel demand on the subway network after disturbances
Chan et al. [31]	WN	Revenue vehicle-miles	Lost service days
Zhang et al. [25]	UN	Throughput, OD connectivity, average reciprocal distance	Ratio of the expected maximum performance that can be accommodated post-failure to the achievable pre-disaster performance
Lu [26]	UN	Importance-impedance-based indicator	Recovery rate
Zhang et al. [32] and Saadat et al. [33]	UN	Network efficiency	Performance loss
Li et al [34]	UN	Weighted sum of nodes' performance	Performance loss
Mudigonda et al. [35]	UN	Travel time, total number of passenger trips	Recovery rate
Chang et al. [29]	UN	Level of service	Performance loss
Chen et al. [36]	UN	Reciprocal of global accessibility indicator, proportion of unaffected passengers	Performance loss

Note: WN = Without constructing network; UN = Undirected network; DN = Directed network.

line 12 caused trains on this line to be delayed for more than 15 min [5]. In January 2020, the COVID-19 outbreak resulted in the shutdown of the Wuhan subway system [6]. These disturbances significantly affected the normal operations of the URT system. Therefore, it is important to assess and enhance the ability of the URT system to respond to disturbances.

The concept of resilience has been widely applied to assess a URT network's ability to respond to disturbances [7]. Resilience stems from the Latin word "resiliere", which means restoration and spring back [8]. In 1973, Holling [9] first used resilience as a metric to assess an ecosystem's ability to respond to external shocks. Thereafter, the concept of resilience was widely applied to assess the abilities of economies [10], social science [11], and supply chains [12] to respond to disturbances. Murray-Tuite proposed a specific definition and a quantitative method to assess the resilience of a transportation system in 2006 [13]. Thus far, researchers have assessed the resilience of road [13–15], railway [16,17], waterway [18], and air transport networks [19]. Different transport modes have distinct definitions of resilience; however, they have the following common features [8]: (1) the ability of a transportation network to maintain functionality under disturbances; and (2) the time and resources required to restore performance after disturbances. For assessing the resilience of a transportation network, existing metrics were divided into three categories: (1) topological, (2) attribute-based, and (3) performance-based metrics. The topological metrics were constructed based on graph properties (e.g., betweenness centrality (BC) [20], average shortest path [21], and network efficiency [22]), and the resilience of a transportation network was assessed by observing the variation in the values of the network's topological metrics before and after disturbances. Attribute- and performance-based metrics were formulated by integrating the network structure and passenger trips jointly. The difference between them was that the attribute-based metrics assessed resilience from some specific properties (e.g., recovery rate [23]), whereas performance-based metrics assessed a transportation network's resilience based on its performance over the entire affected period during the disturbances.

In the past decades, the resilience assessment of URT networks has become increasingly popular. We have listed some studies, which have assessed the resilience of a URT network in Table 1. Studies that do not consider the performance loss during the network recovery phase were excluded. In general, the method for assessing the resilience of a URT network in the existing literature includes the following steps. First, the complex network theory proposed by Watts and Strogatz [24] was widely applied to abstract a URT network as an undirected [25,26] or a directed network [27]. Thereafter, indicators such as network efficiency [28], amount of satisfied travel demand [27], and origination–destination (OD) station connectivity [25] were formulated from the perspective of network structure or passenger travel demand to evaluate the performance of a URT network. Finally, the resilience of a URT network was assessed using the resilience theory (e.g., performance recovery rate [26], and performance loss during the entire affected period [28,29]) based on historical data or simulations.

Although existing research has established a certain foundation for the resilience assessment of a URT network, there are some limitations that have to be addressed: (1) Majority of the studies assess the resilience from the perspective of network structure or passenger travel demand. However, few studies have considered the network structure and passenger travel demand jointly. (2) Node centrality-based attack strategies are widely used to simulate malicious disturbances while assessing a URT network's resilience. The node centrality (e.g., degree centrality and BC) is proposed based on the structure of a URT network, and the passengers' path choice behavior is neglected. (3) Impractical assumptions, such as ignoring the duration of performance degradation and neglecting emergency response time before repair, are considered while applying the resilience triangle to assess the resilience of a URT network.

In this study, we modified the metric for assessing a URT network's resilience to overcome the abovementioned shortcomings. The main contributions of this study are as follows: (1) We have proposed a demand–impedance (DI) indicator that integrates a URT network's structure and passenger travel demand jointly to evaluate the performance of a network. (2) A node centrality, called effective path betweenness (EPB), is formulated by modifying the BC. The EPB considers effective travel paths (ETPs) and passengers' path choice behavior for evaluating the importance of stations in a URT network. (3) A performance curve has been introduced by discussing the durations of the disturbance, response, and recovery phases, and a modified resilience metric has been formulated based on the resilience triangle.

The remainder of this paper is organized as follows: In Section 2, a method for assessing the resilience of a URT network has been formulated based on the DI indicator, EPB, and performance curve. In Section 3, a simulation-based solution algorithm has been proposed to assess the resilience of a URT network. Section 4 implements the proposed method and metric to assess the resilience of the Chengdu subway network during morning peak hours, and some useful suggestions have been proposed. Finally, we have summarized our main findings and future work in Section 5.

2. Method

2.1. Assumption

1. All disturbances occur at the same time and passengers whose paths contain failed stations are affected.
2. The repair work is carried out at the end of disturbances.
3. In the analysis period, new disturbances do not happen during and after the repair process.

2.2. URT network

The URT network is abstracted as an undirected graph $G(V, E)$. $V = \{v_1, v_2, \ldots, v_n\}$ and $E = \{e_1, e_2, \ldots, e_l\}$ denote the sets of URT stations and links, respectively. n and l are the numbers of URT stations and links, respectively. An adjacency matrix $A = [a_{ij}]_{n\times n}$ with binary variables is used to describe the adjacency of stations in G. If stations i and j are connected by a link directly, then a_{ij} and a_{ji} are equal to 1; otherwise a_{ij} and a_{ji} are equal to 0.

2.3. Performance of the URT network

2.3.1. DI indicator

We have proposed a DI indicator, which refers to the network efficiency [22], to evaluate the performance of the URT network. The DI indicator reflects the number of passengers that a URT network can transport within a given time. In the DI indicator, the number of passengers among OD pairs represented as demand does not change during the analysis period, and the impedance is reflected in the travel time among OD pairs. The DI indicator Q of a URT network is computed using Eq. (1):

$$Q = \frac{1}{n(n-1)} \sum_{i\in V} \sum_{j\in V} \frac{v_{ij} \cdot w_{ij}}{t_{ij}}, i \neq j, \tag{1}$$

where v_{ij} is the total number of passenger trips from stations i to j (persons). w_{ij}, $w_{ij} = \sqrt{I_i \cdot I_j}$ denotes the travel importance from stations i to j. I_i and I_j are the importance of stations i and j, respectively, which will be discussed in Section 2.4. t_{ij} represents the weighted average travel time on all ETPs from stations i to j (s), which is computed using Eq. (2):

$$t_{ij} = \sum_{k\in K_{ij}} p_{ij}^k \cdot t_{ij}^k, \tag{2}$$

where K_{ij} is the set of ETPs from stations i to j, (the κ-shortest paths from stations i to j are defined as K_{ij} in this study). κ is the threshold coefficient obtained from a passenger survey. p_{ij}^k denotes the probability of path k being selected, and it is computed based on the stochastic user equilibrium assignment model described in the subsection that follows. t_{ij}^k is the travel time on path k (s).

2.3.2. Stochastic user equilibrium assignment model

A stochastic user equilibrium assignment model incorporating the C-logit model is applied to compute the probabilities of ETPs being selected. Compared to other logit model variants, the C-logit model reflects not only the overlapping effect between paths but also the passengers' travel characteristics. The stochastic user equilibrium assignment model combined with a C-logit model [37] can be expressed as follows:

$$\min Z(v) = \sum_{i\in V} \sum_{j\in V} \sum_{k\in K_{ij}} \frac{v_{ij}^k}{\theta} \cdot \ln(v_{ij}^k) + \sum_{e\in E} \int_0^{v_e} t_e(x)dx + \sum_{i\in V} \sum_{j\in V} \sum_{k\in K_{ij}} v_{ij}^k \cdot w_{ij}^k, \tag{3}$$

$$v_{ij}^{k} = p_{ij}^{k} \cdot v_{ij}, \tag{4}$$

$$v_e = \sum_{i \in V} \sum_{j \in V} \sum_{k \in K_{ij}} v_{ij}^{k} \cdot \delta_{e,k}^{ij}, \tag{5}$$

$$p_{ij}^{k} = \frac{\exp[-\theta \cdot (g_{ij}^{k} + w_{ij}^{k})]}{\sum_{k \in K_{ij}} \exp[-\theta \cdot (g_{ij}^{k} + w_{ij}^{k})]}, \tag{6}$$

$$g_{ij}^{k} = g_{ij}^{k_V} + g_{ij}^{k_E}, \tag{7}$$

$$g_{ij}^{k_V} = \sum_{v_1 \in k_{V_1}} t_{\mathrm{s}}(v_1) + \sum_{v_2 \in k_{V_2}} \mu \cdot [t_{\mathrm{w}}(v_2) + t_{\mathrm{h}}(v_2)] \cdot \left| k_{V_2} \right|^{\zeta}, \tag{8}$$

$$g_{ij}^{k_E} = \sum_{e \in k_E} t_e(x), \tag{9}$$

$$w_{ij}^{k} = \theta \cdot \ln\left(\sum_{o=1}^{|K_{ij}|} \frac{L_{ij}^{k,o}}{\sqrt{L_{ij}^{k} \cdot L_{ij}^{o}}}\right), \tag{10}$$

$$t_e(x) = \begin{cases} 1.3 r_e & v_e \le b_e \\ \left[\dfrac{1.3 b_e + 2.32(v_e - b_e)}{v_e}\right] \cdot r_e & b_e < v_e \le c_e \end{cases}, \tag{11}$$

where v_{ij}^{k} denotes the total number of passenger trips on path k from stations i to j (persons), which is computed using Eq. (4). θ is a parameter that reflects the sensitivity of passengers to the travel time of paths. A higher value of θ implies that passengers are more sensitive to the travel time of the path. v_e represents the total number of passenger trips on link e (persons), which is calculated using Eq. (5). $\delta_{e,k}^{ij}$ is a binary variable. If link e is on path k from stations i to j, then $\delta_{e,k}^{ij} = 1$; otherwise $\delta_{e,k}^{ij} = 0$. $t_e(x)$ represents the perceived travel time of passengers on link e (s), which is calculated using Eq. (11). r_e denotes the running time of trains on link e (s). b_e refers to the number of seats in the trains on link e. c_e represents the transport capacity of trains on link e (persons). w_{ij}^{k} is a common factor of path k, which is calculated using Eq. (10). $L_{ij}^{k,o}$ represents the total length of the common links on paths k and o (m). L_{ij}^{k} and L_{ij}^{o} denote the lengths of paths k and o, respectively (m). g_{ij}^{k} is the generalized travel time on path k from stations i to j, which is calculated using Eq. (7). $g_{ij}^{k_V}$ and $g_{ij}^{k_E}$ are computed using Eqs. (8) and (9), which denote the generalized travel time at stations and links on path k, respectively (s). k_{V_1}, k_{V_2}, and k_E represent the sets of non-transfer stations, transfer stations, and links on path k, respectively. $t_{\mathrm{s}}(v_1)$ refers to the dwell time of trains at the non-transfer station v_1 (s). $t_{\mathrm{w}}(v_2)$ and $t_{\mathrm{h}}(v_2)$ represent the transfer walking time and transfer waiting time at transfer station v_2, respectively (s). We let $t_{\mathrm{h}}(v_2)$ to be half of the line's departure time [38]. μ and ζ are the transfer coefficients.

2.3.3. Travel options of passengers under disturbances

Eq. (2) computes the travel time from stations i to j when a URT network operates normally. However, it cannot be applied to calculate the travel time between an OD pair when the ETPs of that OD pair are affected by disturbances [39,40]. The travel time of affected OD pairs is determined by the travel options of passengers under disturbances, which include waiting at failed stations until stations are repaired (option 1); traveling through alternative paths on the URT network (option 2); discontinuing traveling on the URT network and shifting to other public transport modes (option 3).

1. Option 1

If the duration of a disturbance on a travel path is below the tolerance time of the passenger τ, then passengers (called affected passengers) whose travel paths contain failed stations will wait for recovery at failed stations [26]. The travel time t'_{ij} from stations i to j with option 1 is computed using Eq. (12) (s). $\tilde{t}_{ij}^{k}$ denotes the travel time on path k from stations i to j under disturbances (s), which is calculated using Eq. (13). t_{w} is the waiting time of the passenger owing to disturbances (s). In Eq. (14), D_v calculates the passengers' average waiting time at failed station v before repair (s). $\left\lceil \frac{W_v + A_v \cdot D_v}{C_v} \right\rceil$ returns to the ceiling value of $\frac{W_v + A_v \cdot D_v}{C_v}$, which denotes the number of trains required to transport $W_v + A_v \cdot D_v$ passengers after

repair. As a result, the total passenger waiting time at failed station v for boarding trains after the repair is formulated as $\left\lceil \frac{W_v + A_v \cdot D_v}{C_v} \right\rceil \cdot F_v$.

$$t'_{ij} = \sum_{k \in K_{ij}} p_{ij}^k \cdot \tilde{t}_{ij}^k, \tag{12}$$

$$\tilde{t}_{ij}^k = t_{ij}^k + t_{\mathrm{w}}, \tag{13}$$

$$t_{\mathrm{w}} = D_v + \left\lceil \frac{W_v + A_v \cdot D_v}{C_v} \right\rceil \cdot F_v, \tag{14}$$

where D_v is the disturbance duration at failed station v (s). W_v represents the number of passengers waiting at failed station v when disturbances occur (persons). A_v denotes the passengers' arrival rate at failed station v (persons/s). C_v is the transport capacity of trains stopping at failed station v (persons). F_v represents the time interval between the trains stopping at failed station v (s).

2. Option 2

If the duration of a disturbance on a travel path exceeds the passengers' tolerance time τ and alternative paths exist on the URT network, then the affected passengers choose alternative paths. Several alternative paths may be available among stations in a complex URT network, and passengers choose alternative paths according to their utility [41]. The logit model and its variants have an advantage in expressing passengers' pursuit of utilities; thus, the logit model can be applied to compute the probabilities of alternative paths being chosen by passengers under disturbances. The travel time t'_{ij} of passengers who choose option 2 is expressed as follows [42]:

$$t'_{ij} = \sum_{k \in K'_{ij}} \tilde{p}_{ij}^k \cdot t_{ij}^k, \tag{15}$$

$$\tilde{p}_{ij}^k = \frac{\exp(-\theta \cdot t_{ij}^k)}{\sum_{k \in K'_{ij}} \exp(-\theta \cdot t_{ij}^k)}, \tag{16}$$

where K'_{ij} denotes the set of alternative paths from stations i to j under disturbances. $\tilde{p}_{ij}^k$ is the probability of alternative path k being selected under disturbances.

3. Option 3

If the duration of a disturbance on a travel path exceeds the passengers' tolerance time τ and the affected passengers do not have alternative paths, they often shift to other alternative public transport modes. Subways and buses are the most commonly used public transport modes in China's metropolises (e.g., Beijing, Shanghai, and Chengdu), thus, passengers shift to the bus system when they choose option 3. Passengers' travel time t'_{ij} with option 3 is as follows:

$$t'_{ij} = \frac{d_{ii'}}{v_w} + \varphi \cdot q_{i'j'}, \tag{17}$$

where $d_{ii'}$ is the walking distance from URT station i to bus stop i' (m). Multiple alternative bus stops can be chosen by passengers around URT stations i and j. Thus, we have depicted a flowchart in Fig. 1 to select the origination bus stop i' and destination bus stop j'. Fig. 1 illustrates the assumption that passengers obtain the bus operation information around URT stations i and j based on smartphone applications (e.g., Google map and Baidu map). Malandri et al. considered this assumption in their research [43]. Passengers choose the nearest bus stop to the destination URT station j as the destination bus stop j' according to smartphone applications. Passengers then select the origination bus stop i', which has the minimal travel time to the destination bus stop j' because they tend to arrive at their destinations as soon as possible. v_w is the passengers' walking speed, $v_w = 1.25$ m/s. φ is a penalty coefficient for estimating the penalty time from a URT system to a bus system, $\varphi = 1.1$ [44]. $q_{i'j'}$ is the shortest travel time from the origination bus stop i' to the destination bus stop j' (s).

2.4. Importance of stations

Protecting critical stations is of practical significance for strengthening the URT network's ability to respond to disturbances. Critical stations are identified by node centrality, in which the passengers' path choice behavior is always neglected. BC, which is one of the most popularly applied node centralities, is calculated using Eq. (18). BC only considers the shortest paths among stations, and it does not distinguish the probabilities of paths being selected for evaluating a station's importance. However, all ETPs can be chosen by passengers on a URT network in daily operation, and the probability of each ETP being selected is different. Hence, a node centrality called EPB is proposed by modifying Eq. (18).

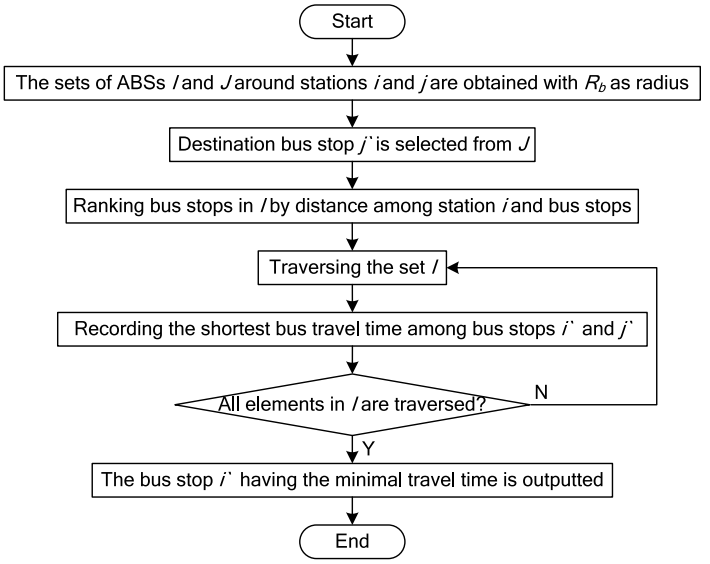

Fig. 1. Flowchart to select origination bus stops. Note: ABSs = Alternative Bus Stops.

The EPB I_o of station o is computed using Eq. (19). In particular, BC and EPB are equal only when passengers travel through the shortest paths on a URT network, and the probabilities of the shortest paths being selected are not distinguished.

$$B_o = \sum_{i \neq o \neq j \in V} \frac{\sigma_{ij}(o)}{\sigma_{ij}}, \tag{18}$$

$$I_o = \sum_{i \neq o \neq j \in V} \frac{\eta_{ij}^*(o)}{\eta_{ij}} = \sum_{i \neq o \neq j \in V} \frac{1}{\eta_{ij}} \sum_{k \in K_{ij}} p_{ij}^k \cdot \delta_{k,o}, \tag{19}$$

where B_o represents the BC of station o; $\sigma_{ij}(o)$ denotes the number of shortest paths from stations i to j via station o. σ_{ij} and η_{ij} are the numbers of shortest paths and ETPs from stations i to j, respectively. $\eta_{ij}^*(o)$ represents the weighted number of ETPs from stations i to j via station o, the weights of ETPs being equal to the probabilities of ETPs being selected by passengers, $\eta_{ij}^*(o) = \sum_{k \in K_{ij}} p_{ij}^k \cdot \delta_{k,o}$. $\delta_{k,o}$ is a binary variable. If path k contains station o, then $\delta_{k,o} = 1$; otherwise $\delta_{k,o} = 0$.

2.5. Resilience of the URT network

2.5.1. Attack strategy

A URT network can be affected by station or link failures. We considered only station failure in this study. The critical reason is that stations are open to the public and can easily be damaged by attacks and hazards [32]. In daily operations, the disturbances that lead to station failure include random (e.g., natural disasters, equipment failures) and malicious disturbances (e.g., terrorist attacks). In this study, to simulate random disturbances, the stations are randomly selected for removal; and to simulate malicious disturbances, the most important stations are first identified via EPB and are later selected for removal.

Disturbances that lead to various station failure severities are considered while simulating station failure. In general, greater passenger trips at a station imply a higher value of failure severity when the station fails owing to disturbances [45]. Therefore, L_i, which is proportional to the total number of passenger trips at station i, is proposed to measure the failure severity of station i. $L_i = 0$ denotes that station i is in normal operation, and a higher value of L_i implies a greater failure severity of station i. Furthermore, a station may have a greater failure severity under malicious disturbances when compared to that under random disturbances, because the former is more harmful to a URT system than the latter. After defining L_i, station i's repair duration Y_i (s), which is proportional to L_i, is computed using Eq. (20).

$$Y_i = 60\vartheta \cdot L_i, \tag{20}$$

where ϑ is a coefficient that reflects the relationship between L_i and Y_i. A URT system with a greater rescue ability repairs the failed station i in a shorter time when L_i is fixed. Therefore, ϑ is related to a URT system's rescue ability, and a smaller ϑ represents greater rescue ability.

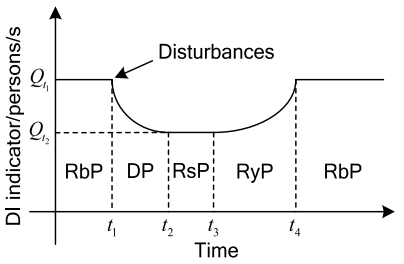

Fig. 2. DI indicators of a URT network during the attack and repair processes. Note: RbP = Reliable Phase, DP = Disturbance Phase, RsP = Response Phase, RyP = Recovery Phase.

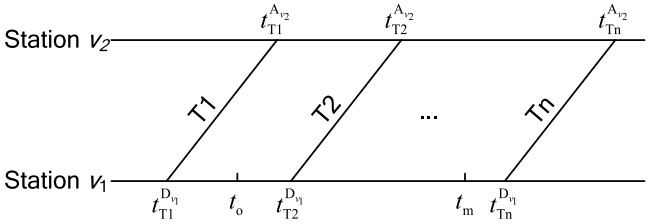

Fig. 3. Part of the schedule diagram of a URT line.

2.5.2. Modified resilience metric

The DI indicators of a URT network during the attack and repair processes are depicted in Fig. 2. From Fig. 2, we can see that the URT network is attacked by disturbances at t_1 and its DI indicator drops to the lowest level at t_2. Thereafter, the repair work is carried out at t_3 and the work is completed at t_4. The URT network depicted in Fig. 2 is divided into reliable, disturbance, response, and recovery phases according to its DI indicator at different moments. Let us discuss the durations of the disturbance, response, and recovery phases in detail.

1. Duration of the disturbance phase

Disturbances affect the operations of trains whose routes include failed stations. As a result, passengers who intend to board or have already boarded the affected trains are affected. In China, trains operate according to schedules. A small part of the schedule diagram of a URT line is depicted in Fig. 3. In Fig. 3, the horizontal and slanted lines represent the URT stations and trains, respectively. $t_{\mathrm{T1}}^{\mathrm{D}_{v_1}}$ and $t_{\mathrm{T1}}^{\mathrm{A}_{v_2}}$ denote train T1's departure time at station v_1 and arrival time at station v_2, respectively, $t_{\mathrm{T1}}^{\mathrm{A}_{v_2}} > t_{\mathrm{T1}}^{\mathrm{D}_{v_1}}$.

It is assumed that a disturbance occurs at station v_1 at time t_{o} and the failed station is repaired at t_{m} (as depicted in Fig. 3). The duration of the disturbance phase is $t_{\mathrm{T2}}^{\mathrm{D}_{v_1}} - t_{\mathrm{o}}$. This is because the URT network normally operates from $t_{\mathrm{T1}}^{\mathrm{D}_{v_1}}$ to t_{o}. The disturbance does not affect the operation of train T1. Train T2 is the first train to get affected after the disturbance. Passengers who intend to board or have already boarded train T2 are affected, and the DI indicator of the URT network is considered to drop to the lowest level at $t_{\mathrm{T2}}^{\mathrm{D}_{v_1}}$. We assume that t_{o} follows a uniform distribution $U(t_{\mathrm{T1}}^{\mathrm{D}_{v_1}}, t_{\mathrm{T2}}^{\mathrm{D}_{v_1}})$, because of the possibility of a disturbance to occur at any time between $t_{\mathrm{T1}}^{\mathrm{D}_{v_1}}$ and $t_{\mathrm{T2}}^{\mathrm{D}_{v_1}}$ [46]. The expectation $E(t_{\mathrm{o}})$ of t_{o} is $(t_{\mathrm{T1}}^{\mathrm{D}_{v_1}} + t_{\mathrm{T2}}^{\mathrm{D}_{v_1}})/2$. Hence, we apply the expectation of $t_{\mathrm{T2}}^{\mathrm{D}_{v_1}} - t_{\mathrm{o}}$ to estimate the duration of the disturbance phase when station v_1 fails.

$$T_1 = E\left(t_{\mathrm{T2}}^{\mathrm{D}_{v_1}} - t_{\mathrm{o}}\right) = t_{\mathrm{T2}}^{\mathrm{D}_{v_1}} - E\left(t_{\mathrm{o}}\right) = \frac{t_{\mathrm{T2}}^{\mathrm{D}_{v_1}} - t_{\mathrm{T1}}^{\mathrm{D}_{v_1}}}{2} = \frac{F_{v_1}}{2} \tag{21}$$

If the number of failed stations exceeds 1, then the duration of the disturbance phase can be expressed as follows:

$$T_1 = \max_{v \in V_1} \left\{ \frac{F_v}{2} \right\}, \tag{22}$$

where V_1 denotes the set of failed stations.

2. Duration of the response phase

The duration of the response phase is mainly affected by the emergency response time of the URT system. In China, the law of the People's Republic of China on work safety [47] requires that the duration of emergency response for a URT operation department cannot exceed a specific time. That is, the emergency response time is fixed for a URT system. Hence, we defined the duration of response phase T_2 as a constant:

$$T_2 = t_{\mathrm{r}}, \tag{23}$$

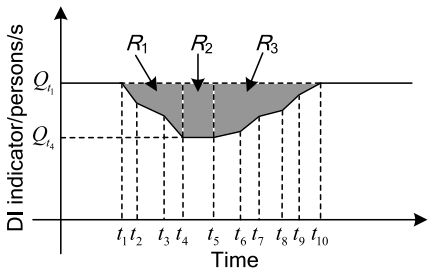

Fig. 4. A URT network's DI indicator during attack and repair processes.

where t_r is the emergency response time of the URT system (s). Different URT systems have different values, we set $t_r = 120$ s in this study.

3. Duration of the recovery phase

The duration of the recovery phase relates to the station failure severity and the recovery strategy of the URT system. The preference recovery strategy [38], wherein failed stations are repaired sequentially according to their EPB, is applied herein to repair the disrupted URT network. The duration of the recovery phase T_3 is as follows:

$$T_3 = t_p, \tag{24}$$

where t_p represents the total repair time that is determined by the preference repair strategy (s).

The performance curve of a URT network during the attack and repair processes is depicted in Fig. 4 according to the durations of the disturbance, response, and recovery phases. The shaded area depicted in Fig. 4 denotes the performance loss of the URT network under disturbances. According to the resilience triangle [32], the retained performance during the attack and repair processes is used as a resilience metric R:

$$R = 1 - (R_1 + R_2 + R_3), \tag{25}$$

where R_1, R_2, and R_3 represent the performance losses during the disturbance, response, and recovery phases, respectively, which are calculated using Eqs. (26)–(28).

$$R_1 = \frac{\int_{t_o}^{t_o+T_1}[Q_0 - Q(t)]dt}{Q_0 T_1}, \tag{26}$$

$$R_2 = \frac{T_2 \cdot (Q_0 - Q_{t_o+T_1})}{Q_0 \cdot T_2}, \tag{27}$$

$$R_3 = \frac{\int_{t_o+T_1+T_2}^{t_o+T_1+T_2+T_3}[Q_0 - Q(t)]dt}{Q_0 T_3}, \tag{28}$$

where t_o is the moment when disturbances occur (s). For ease of calculation, we let $t_o = 0$ s. Q_0 denotes the DI indicator of a normally operating URT network (persons/s). $Q(t)$ represents the DI indicator of a URT network at time t (persons/s).

3. Solution algorithm

The resilience of a URT network is assessed based on the simulation. At first, the ETPs on a URT network are generated using the pseudocodes listed in Table 2. Studies that apply the depth-first search algorithm and Floyd algorithm are sufficient, and the application details are listed in [48,49], respectively. Secondly, the DI indicator of a normally operating URT network is computed after the passenger trip assignment. Thirdly, the stations are removed and re-added to the URT network during the attack and repair simulations. The curve depicted in Fig. 4 is obtained by calculating the DI indicator of the URT network during the attack and repair processes. Lastly, the modified resilience metric of the URT network is computed. The algorithm flowchart for assessing the resilience of a URT network is depicted in Fig. 5. The research on using the method of successive weighted average (MSWA) algorithm to solve the passenger trip assignment model is sufficient, and the details of applying the MSWA algorithm are described in [50].

The dotted box depicted in Fig. 5 is used to calculate the DI indicator of the URT network under disturbances. The ETPs on a URT network are updated by programming the pseudocode listed in Table 3. Thereafter, the DI indicator of a disrupted URT network is calculated by the complete scanning of all OD pairs.

Table 2
Pseudocode for generating ETPs on a normally operating URT network.

Algorithm I: Generating ETPs on a normally operating URT network

Input: κ //Threshold coefficient.
P //Set of travel paths among all OD pairs, which is obtained by applying a depth-first search algorithm.
PT //Set of travel time on all travel paths, which is obtained by applying a depth-first search algorithm.
ST //Set of shortest travel time among all OD pairs, which is obtained by applying a Floyd algorithm.
Output: K_{ij} //Set of ETPs.

```
1. for i = 1 to length[P] do
2.   for j = 1 to length[P] do
3.     if P_ij ≠empty do                    //Set of travel paths is not empty.
4.       s = 1;
5.       for p in P_ij do                   //Traversing set.
6.         if PT_ij (p) ≤ κ · ST_ij do      //Path k's travel time is below the threshold time.
7.           K_ij[s] = p;                   //Recording path k as an ETP.
8.           s = s + 1;
9.         endif
10.      endfor
11.    endif
12.  endfor
13. endfor
```

Table 3
Pseudocode for updating ETPs on a disrupted URT network.

Algorithm II: Updating ETPs on a disrupted URT network

Input: A //A URT network's adjacency matrix.
τ //Passengers' tolerance time.
V_1 //Set of failed stations.
T_d //Set of failed time at stations.
K_{ij} //Set of ETPs under normal operations.
Output: K_{ij}^* //Set of updated ETPs.

```
1. for i = 1 to length[A] do
2.   for j = 1 to length[A] do
3.     if K_ij ≠empty do                    //Set of ETPs is not empty.
4.       s = 1;
5.       for k in K_ij do                   //Traversing the set of ETPs.
6.         if V_1 ∩ k ≠empty do             //Path k contains failed stations.
7.           t = max(T_d^*);                //The greatest failed time on path k is recorded.
8.           if t ≤ τ do                    //Path k's failed time does not exceed τ.
9.             K_ij^*[s] = k;               //The set of ETPs is updated.
10.            s = s + 1;
11.          endif
12.        endif
13.      endfor
14.    endif
15.  endfor
16. endfor
```

4. Implementation

4.1. Chengdu subway

4.1.1. Chengdu subway network

Chengdu is the capital of Sichuan province and the twelfth city that operates a URT system in mainland China. The effectiveness of the proposed method and metric are verified by applying them to the Chengdu subway network in April 2019. Fig. 6 depicts the six operation lines, 156 stations (including 14 transfer stations), and 166 links in the Chengdu subway in April 2019.

4.1.2. Data preparation

The data of automatic fare collection, which were obtained from a manager in the Chengdu subway, are processed before assessing the network's resilience. After data processing, passenger OD trips during the morning peak hours are obtained. We obtained train operation data (e.g., train schedule on each line) and transfer walking time at transfer stations

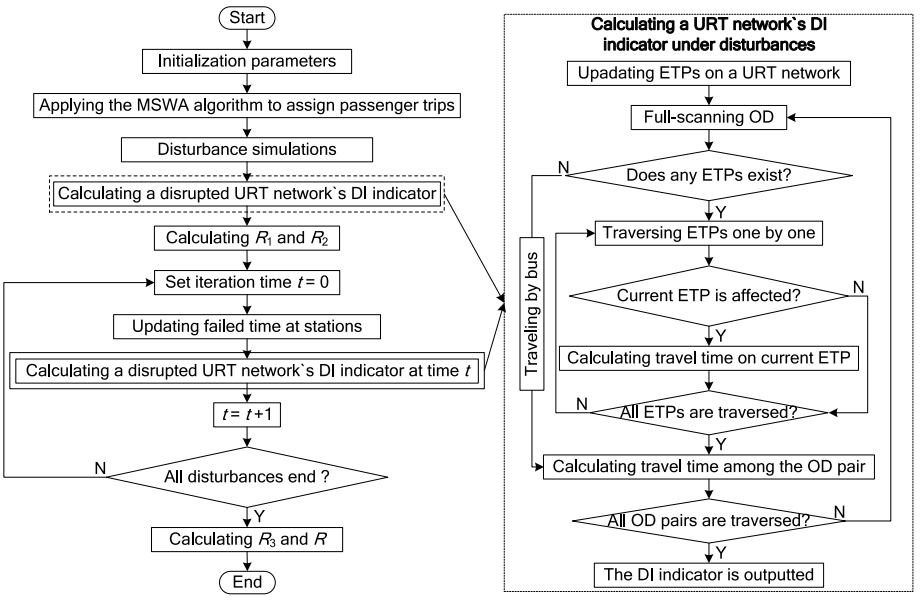

Fig. 5. Flowchart for assessing a URT network's resilience.

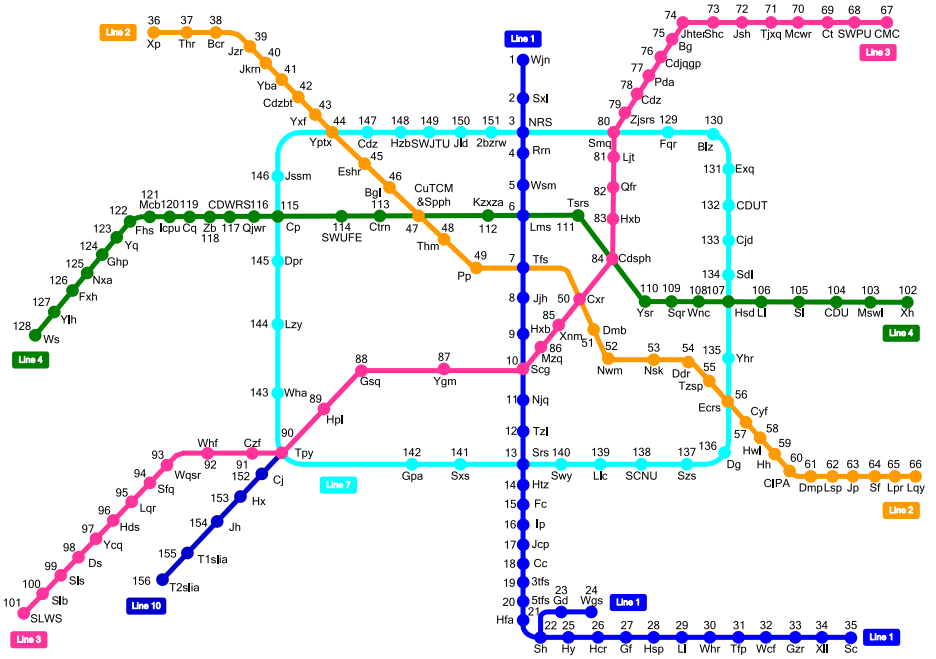

Fig. 6. Chengdu subway network in April 2019.

from a Chengdu subway manager. The bus operation data (bus routes, location of bus stops, and running time among bus stops) were crawled by processing Amap data [51] with Python.

The parameters used in Fig. 5 are determined as follows: Passengers' perception parameter $\theta = 1.866$, transfer coefficients $\mu = 1.1$, $\zeta = 0.5$ according to [38]; Passengers' tolerance time $\tau = 5$ min and threshold coefficient $\kappa = 1.3$ according to a passenger survey. The maximal distance from a bus stop to a URT station is $R_b = 400$ m.

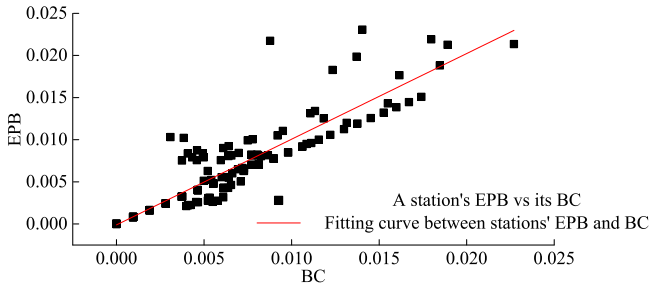

Fig. 7. Stations' EPB versus their BC on the Chengdu subway network.

Table 4
Number of affected passengers and DI indicator reduction caused by the failures of five critical stations identified with EPB and BC.

Node centrality	NoAP	DI indicator reduction ($D = 60$ s)	DI indicator reduction ($D = 360$ s)
EPB	181,216 persons	8.256×10^{-7} persons/s	2.644×10^{-5} persons/s
BC	168,539 persons	3.452×10^{-6} persons/s	2.386×10^{-5} persons/s

Note: NoAP = Number of affected passengers.

4.2. Importance of stations

The BC and EPB of stations on the Chengdu subway are calculated, and the relationship between the EPB and BC of stations is depicted in Fig. 7. The correlation coefficient between the EPB and BC of stations on the Chengdu subway is 0.901. This result implies that a station's EPB is positively related to its BC, and a station with a higher value of BC tends to have a higher EPB. The number of affected passengers and DI indicator reduction caused by the failures of five critical stations identified by EPB and BC are listed in Table 4. Passenger trip assignment result indicates that the critical stations identified with EPB are more important than the critical stations identified with BC in terms of transporting passengers. When the disturbance duration is less than the passengers' tolerance time (5 min), the DI indicator reduction caused by the failures of critical stations identified with EPB and BC is relatively small. The DI indicator reduction owing to failures of critical stations identified with EPB is smaller because the total arrival rate of passengers at five critical stations identified with EPB (2.194 persons/s) is smaller than that of stations identified with BC (2.686 persons/s). However, the failures of critical stations cause a significant reduction in the DI indicators when the disturbance duration exceeded 5 min. The DI indicator reduction owing to the failures of critical stations identified with EPB is greater than that identified with BC. Based on the above discussion, we can see that EPB is more effective for identifying critical stations in a URT network when compared to BC.

4.3. Resilience of the Chengdu subway network

4.3.1. Performance of the Chengdu subway network

The values of the Chengdu subway network's DI indicator and the total number of passenger trips on the network during the operation hours are computed and depicted in Fig. 8. The results indicate that the DI indicator of the Chengdu subway network is proportional to the total number of passenger trips on the network. According to Eq. (1), a URT network's DI indicator equals the weighted sum of the OD pairs' DI indicator. Hence, the effectiveness of a URT network's DI indicator can be verified by illustrating the effectiveness of the DI indicators among the OD pairs. The Sxl station (station number is 2) on line 1 is considered as an example to illustrate the effectiveness of the DI indicator from the Sxl station to other stations on line 1. The normalized DI indicator and normalized efficiency from the Sxl station to another station on line 1 (station numbers from 1 to 35) are depicted in Fig. 9. The correlation coefficient between the normalized DI indicator and normalized efficiency depicted in Fig. 9 is 0.237, which implies that the normalized DI indicator and normalized efficiency have a low correlation. The efficiency among stations is inversely related to travel time among stations, and it does not consider the total number of passenger trips among stations. The DI indicator is proportional to the total number of passenger trips among other stations. Greater passenger trips among stations imply a higher DI indicator. The main function of a URT network is to transport passengers; thus, passenger trips are considered important for evaluating the performance of a URT network. Here, passenger trips among OD pairs and weighted average travel time on ETPs are considered in the DI indicator, which increase the effectiveness of the DI indicator when compared to the network efficiency while evaluating a URT network's performance.

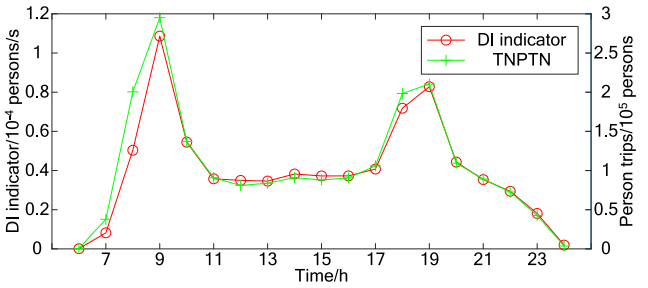

Fig. 8. Values of the network's DI indicator and the total number of passenger trips on the network during the operation hours. Note: TNPTN = Total Number of Passenger Trips on the Network.

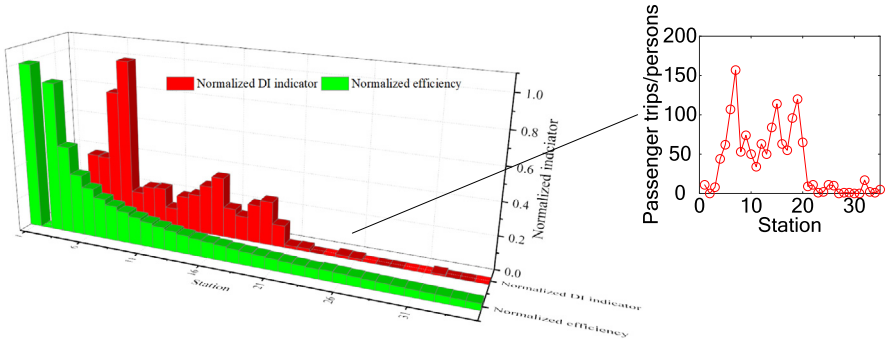

Fig. 9. Normalized DI indicator and normalized efficiency from Sxl station to other stations on line 1.

Table 5
Failure severities and passengers' arrival rates of stations chosen to simulate random and malicious disturbances.

Random disturbances						Malicious disturbances					
Station	FS	PAR	Station	FS	PAR	Station	FS	PAR	Station	FS	PAR
Sl	0.934	0.330	Yxf	3.232	0.826	Tpy	2.113	0.464	CuTCM&Spph	9.967	0.628
Thm	1.908	0.200	Wsm	3.547	0.612	Cp	3.252	0.837	Htz	11.705	0.820
Nxa	2.194	0.411	Tsrs	3.773	0.344	Srs	4.476	0.401	Lms	13.102	0.537
Sxs	2.228	0.368	Fc	3.828	0.782	Cdsph	5.521	0.648	Tfs	13.594	0.256
Jjh	2.449	0.191	Lms	3.976	0.537	Scg	6.808	0.605	Cxr	19.195	0.395

Note: FS = Failure Severity; PAR = Passengers' Arrival Rate.

4.3.2. Chengdu subway network's resilience

1. Simulation scenarios

The failure severities and passengers' arrival rates (persons/s) of stations that are chosen to simulate random and malicious disturbances during morning peak hours are listed in Table 5.

2. Resilience assessment of the Chengdu subway network

The DI indicator of the Chengdu subway network during the attack and repair processes under random and malicious disturbances is depicted in Fig. 10. The performance curve in Fig. 10 is more consistent with the real operation of the Chengdu subway network during disturbances than the widely applied performance curve listed in [32]. The performance curve can describe the change in a network's DI indicator in detail, and thus, it comprehensively assesses the resilience of a URT network. The resilience of the Chengdu subway network is computed using Eqs. (25)–(28). The resilience of the Chengdu subway network under malicious disturbances is 0.840, which is lower than the resilience of the Chengdu subway network under random disturbances (0.918). Malicious disturbances are more harmful to the resilience of the Chengdu subway network than random disturbances. Thus, Chengdu subway operators need to focus on the operations of critical stations (such as Tpy station, which is the bridge node among Shuangliu District and downtown Chengdu, Cp station, which connects Wenjiang District and downtown Chengdu) to avoid network paralysis caused by the failures of critical stations.

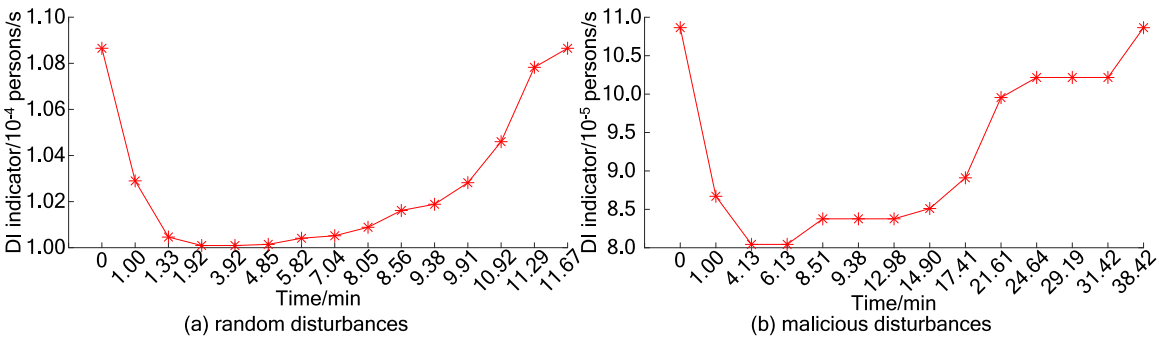

Fig. 10. Network's DI indicator during attack and repair processes under random and malicious disturbances.

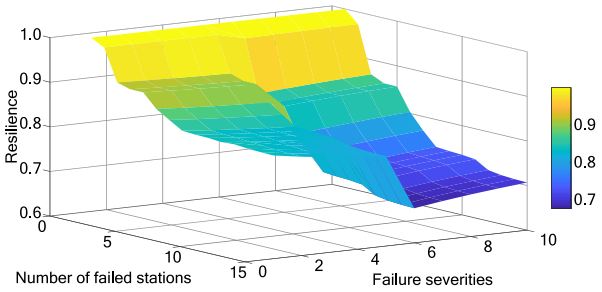

Fig. 11. Relation among resilience, number of failed stations, and failure severities.

Table 6
The values of failure severities should not be exceeded to guarantee that $R > 0.9$ when the number of failed stations is different.

Number of failed stations	Values of failure severities should not exceed	Number of failed stations	Values of failure severities should not exceed
1	10	9	0
2	10	10	0
3	5	11	0
4	1	12	0
5	1	13	0
6	0	14	0
7	0	15	0
8	0	–	–

4.3.3. Sensitivity on parameters on Chengdu subway network's resilience

In this subsection, we shall discuss the influences of the parameters on the resilience of the Chengdu subway network using the control variate method. By considering station failure in the Chengdu subway caused by malicious disturbances as an example, its resilience under a different number of failed stations with different failure severities is depicted in Fig. 11.

As illustrated in Fig. 11 ($t_r = 120$ s, $\tau = 300$ s, and $\vartheta = 1$), the network's resilience is inversely proportional to the number of failed stations when the values of failure severities are fixed. More failed stations imply a smaller value of resilience. When the number of failed stations is fixed, greater failure severities lead to lower resilience. The Chengdu subway network has higher resilience when the failure severity is less than 5 (i.e., the disturbance duration is 5 min).

To maintain the high resilience of the Chengdu subway network, i.e., to guarantee that $R > 0.9$, the values of failure severities that should not exceed are listed in Table 6, when the number of failed stations is different. To guarantee $R > 0.9$, the number of failed stations that should not be exceeded is listed in Table 7, when the values of failure severities are different. Tables 6 and 7 provide a monitoring failure severity and a monitoring number of failure stations, respectively, to ensure the high resilience of the Chengdu subway network when station failure occurs, which helps operators monitor the operations of the network to maintain its high resilience.

The effects of parameters t_r, τ, and ϑ on the Chengdu subway network's resilience are displayed in Fig. 12. Fig. 12(a) ($\tau = 300$ s, and $\vartheta = 1$) depicts that the network's resilience is inversely proportional to t_r. The fitting equation between R and t_r is $R = -0.009t_r + 0.858$. This indicates that the network's resilience can be improved effectively by shortening the emergency response time, and a 1 s reduction in emergency response time can increase the network's resilience by

Table 7
The numbers of failed stations should not be exceeded to guarantee that $R > 0.9$ when the values of failure severities are different.

Values of failure severities	Number of failed stations should not exceed	Values of failure severities	Number of failed stations should not exceed
1	5	6	2
2	5	7	2
3	3	8	2
4	3	9	2
5	2	10	2

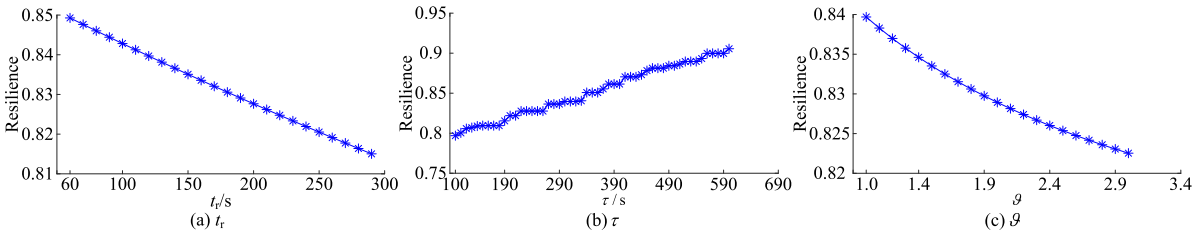

Fig. 12. Effects of parameters t_r, τ, and ϑ on network resilience.

0.009. To reduce the emergency response time, an information-sharing platform that integrates governments, operators, passengers, and public safety agencies should be established in the Chengdu subway system. This platform conveys information efficiently and thus promotes operators to make correct decisions in a shorter time.

Fig. 12(b) ($t_r = 120$ s, and $\vartheta = 1$) indicates that the network's resilience increases with an increase in passengers' tolerance time. When $\tau = 100$ s, the network's resilience is 0.797, whereas its resilience is 0.906 when $\tau = 600$ s. Therefore, the operators can take the following measures to enhance the network's resilience. At first, they need to provide high-quality transportation services (e.g., clean train carriages and friendly passenger inquiry services) to passengers. Secondly, the travel guidance information should be announced promptly through broadcasting and smartphone applications, which help passengers to choose reasonable paths when they need to detour. Finally, operators can temporarily change the train routes to evacuate trapped passengers.

Fig. 12(c) ($t_r = 120$ s, $\tau = 300$ s) illustrates that a greater ϑ implies a smaller value of resilience, and the relation between R and ϑ is $R = -0.008\vartheta + 0.847$. This implies that improving a system's emergency rescue ability can effectively enhance the resilience of the network. For instance, building professional repair teams in the Chengdu subway system to efficiently carry out repair work. The skills of repair teams can be improved by organizing regular emergency rescue drills. Furthermore, operators can seek help from public safety agencies (e.g., the fire and rescue department) when the disturbances are serious.

5. Conclusion

In this study, the resilience of a URT network is assessed. Considering the efficiency of a URT network in transporting passengers, an indicator called the DI indicator is proposed to evaluate the performance of a URT network. By considering a URT network's ETPs and passengers' path choice behavior, a node centrality called EPB is proposed to measure the importance of stations. The performance curve of a URT network during the attack and repair processes has been depicted using the DI indicator, and a modified resilience metric has been formulated based on the performance curve and resilience triangle. Finally, the proposed model and metrics are implemented in the Chengdu subway network. The correlation coefficient between the stations' EPB and BC is 0.901 on the Chengdu subway network. EPB provides a more effective assessment of stations' importance when compared to BC, by considering the importance of stations for transporting passengers and the effect of the stations' failure on a URT network's performance. The DI indicator is considered more suitable for evaluating the network's performance than network efficiency because it can effectively reflect the effect of passenger trips among stations on the network's performance. The proposed performance curve is more consistent with the real operation of the Chengdu subway system during disturbances, and it comprehensively assesses the resilience of the network. The Chengdu subway network possesses greater resilience under random disturbances than under malicious disturbances. Based on the sensitivity analysis of the network's resilience assessment, several practical suggestions involving the management of disturbances, shortening emergency response time, providing passenger services, and improving emergency rescue ability are provided for the management of the Chengdu subway system under disturbances.

Although the model and metric are only verified with the Chengdu subway network, they can be applied to other URT networks worldwide. In future works, we will further modify the resilience metric and propose a weighted resilience metric by considering the importance of different phases (disturbance, response, and recovery phases).

CRediT authorship contribution statement

Jinqu Chen: Methodology, Investigation, Software, Writing – original draft. **Jie Liu:** Software, Data curation, Visualization. **Qiyuan Peng:** Conceptualization, Project administration, Writing – review & editing. **Yong Yin:** Funding acquisition, Writing – review & editing.

Declaration of competing interest

The authors declare that they have no known competing financial interests or personal relationships that could have appeared to influence the work reported in this paper.

Acknowledgments

This work was supported by the National Key R&D Program of China [2017YFB1200700].

References

[1] China Association of Metros, Annual statistics and analysis report on urban rail transit in 2020, 2021.
[2] Y. Yang, Causes of derailment of a train in the Kunming subway system has been identified, 2013, https://www.ynfzb.cn/trafficsafery/xianchangbaodao/178700.shtml. (Accessed 5 July 2020).
[3] Wangyi, A stampede disturbance happens in the Shenzhen subway, 2015, https://news.163.com/photoview/00AP0001/88680.html. (Accessed 5 July 2020).
[4] X. Yang, Railroad turnouts failure has been repaired, 2018, http://www.huaxia.com/zjsx/xwsc/2018/01/5596596.html. (Accessed 5 July 2020).
[5] D. Wang, Signal equipment failure in Shanghai subway line 12 has been repaired, 2019, https://society.huanqiu.com/article/9CaKrnKgUkG. (Accessed 5 July 2020).
[6] M. Yu, Wuhan's bus, subway, ferry, and passenger transport will shut down from the January 23, 2020, 2020, http://sd.iqilu.com/v7/share/article/6312645. (Accessed 5 July 2020).
[7] N. Besinovic, Resilience in railway transport systems: A literature review and research agenda, Transp. Rev. 2020 (2020) 1–22, http://dx.doi.org/10.1080/01441647.2020.1728419.
[8] Y. Zhou, J. Wang, Y. Hai, Resilience of transportation systems: Concepts and comprehensive review, IEEE Trans. Intell. Transp. 12 (2019) 4262–4276, http://dx.doi.org/10.1109/TITS.2018.2883766.
[9] C.S. Holling, Resilience and stability of ecological systems, Annu. Rev. Ecol. Syst. 4 (1973) 1–23, http://dx.doi.org/10.1146/annurev.es.04.110173.000245.
[10] A. Rose, S. Liao, Modeling regional economic resilience to disasters: A computable general equilibrium analysis of water service disruptions, J. Reg. Sci. 45 (2005) 75–112, http://dx.doi.org/10.1111/j.0022-4146.2005.00365.x.
[11] W.N. Adger, Social and ecological resilience: Are they related? Prog. Hum. Geog. 24 (2000) 347–364, http://dx.doi.org/10.1191/030913200701540465.
[12] J. Wang, R. Dou, R.R. Muddada, W. Zhang, Management of a holistic supply chain network for proactive resilience: Theory and case study, Comput. Ind. Eng. 125 (2018) 668–677, http://dx.doi.org/10.1016/j.cie.2017.12.021.
[13] P.M. Murray-Tuite, A comparison of transportation network resilience under simulated system optimum and user equilibrium conditions, Proc. Winter Simul. Conf. 1 (2006) 1398–1405, http://dx.doi.org/10.1109/WSC.2006.323240.
[14] B.K. Bhavathrathan, G.R. Patil, Quantifying resilience using a unique critical cost on road networks subject to recurring capacity disruptions, Transp. Transp. Sci. 11 (2015) 836–855, http://dx.doi.org/10.1080/23249935.2015.1087230.
[15] T.Y. Liao, T.Y. Hu, Y.N. Ko, A resilience optimization model for transportation networks under disasters, Nat. Hazards 93 (2018) 469–489, http://dx.doi.org/10.1007/s11069-018-3310-3.
[16] L. Collis, F. Schmid, A. Tobias, Managing incidents in a complex system: A railway case study, Cogn. Technol. Work 26 (2014) 171–185, http://dx.doi.org/10.1007/s10111-013-0255-x.
[17] Y. Zhu, K. Ozbay, K. Xie, H. Yang, Using big data to study resilience of taxi and subway trips for hurricanes sandy and irene, Transp. Res. Rec. 2599 (2016) 70–80, http://dx.doi.org/10.3141/2599-09.
[18] S. Hosseini, K. Barker, Modeling infrastructure resilience using Bayesian networks: A case study of inland waterway ports, Comput. Ind. Eng. 93 (2016) 252–266, http://dx.doi.org/10.1016/j.cie.2016.01.007.
[19] K.L. Clark, U. Bhatia, E.A. Kodra, A.R. Ganguly, Resilience of the U.S national airspace system airport network, IEEE Trans. Intell. Transp. Syst. 19 (2018) 3785–3794, http://dx.doi.org/10.1109/TITS.2017.2784391.
[20] H. Wang, J. Huang, X. Xu, Y. Xiao, Damage attack on complex networks, Physica A 408 (2014) 134–148, http://dx.doi.org/10.1016/j.physa.2014.04.001.
[21] N. Goldbeck, P. Angeloudis, W.Y. Ochieng, Resilience assessment for interdependent urban infrastructure systems using dynamic network flow models, Reliab. Eng. Syst. Saf. 188 (2019) 62–79, http://dx.doi.org/10.1016/j.ress.2019.03.007.
[22] C.G. Ghedini, C.H.C. Ribeiro, Rethinking failure and attack tolerance assessment in complex networks, Physica A 390 (2011) 4684–4691, http://dx.doi.org/10.1016/j.physa.2011.07.006.
[23] M. Mojtahedi, S. Newton, J. Von Meding, Predicting the resilience of transport infrastructure to a natural disaster using Cox's proportional hazards regression model, Nat. Hazards 85 (2017) 1119–1133, http://dx.doi.org/10.1007/s11069-016-2624-2.
[24] D.J. Watts, S.H. Strogatz, Collective dynamics of 'small-world' networks, Nature 6684 (1998) 440–442, http://dx.doi.org/10.1038/30918.
[25] X. Zhang, E. Miller-Hooks, K. Denny, Assessing the role of network topology in transportation network resilience, J. Transp. Geogr. 46 (2015) 35–45, http://dx.doi.org/10.1016/j.jtrangeo.2015.05.006.
[26] Q. Lu, Modeling network resilience of rail transit under operational incidents, Transp. Res. A 117 (2018) 227–237, http://dx.doi.org/10.1016/j.tra.2018.08.015.
[27] J.G. Jin, L.C. Tang, L. Sun, D.H. Lee, Enhancing metro network resilience via localized integration with bus services, Transp. Res. E 63 (2014) 17–30, http://dx.doi.org/10.1016/j.tre.2014.01.002.
[28] Y. Saadat, B.M. Ayyub, Y. Zhang, D. Zhang, H. Huang, Resilience of metrorail networks: Quantification with Washington, DC as a case study, ASCE-ASME J. Risk Uncert. Eng. Syst. B Mech. Eng. 5 (2019) 041011, http://dx.doi.org/10.1115/1.4044038.

[29] J.S. Chang, D. Juang, S. Jun, H. Oh, Resilience conceptual framework for assessing the performance of transit service, Int. J. Urban Sci. 24 (2020) 339–353, http://dx.doi.org/10.1080/12265934.2019.1687319.
[30] A. Cox, F. Prager, A. Rose, Transportation security and the role of resilience: A foundation for operational metrics, Transp. Policy 18 (2011) 307–317, http://dx.doi.org/10.1016/j.tranpol.2010.09.004.
[31] R. Chan, J.L. Schofer, Measuring transportation system resilience: Response of rail transit to weather disruptions, Nat. Hazards Rev. 17 (2016) 05015004, http://dx.doi.org/10.1061/(ASCE)NH.1527-6996.0000200.
[32] D.M. Zhang, F.F. Du, H.W. Huang, F. Zhang, B.M. Ayyub, M. Beer, Resiliency assessment of urban rail transit networks: Shanghai metro as an example, Saf. Sci. 106 (2018) 230–243, http://dx.doi.org/10.1016/j.ssci.2018.03.023.
[33] Y. Saadat, B.M. Ayyub, Y. Zhang, D. Zhang, H. Huang, Resilience-based strategies for topology enhancement and recovery of metrorail transit networks, ASCE-ASME J. Risk Uncertain. Eng. Syst. A Civ. Eng. 6 (2020) 04020017, http://dx.doi.org/10.1061/AJRUA6.0001057.
[34] M. Li, H. Wang, H. Wang, Resilience assessment and optimization for urban rail transit networks: A case study of Beijing subway network, IEEE Access 7 (2019) 71221–71234, http://dx.doi.org/10.1109/ACCESS.2019.2919105.
[35] S. Mudigonda, K. Ozbay, B. Bartin, Evaluating the resilience and recovery of public transit system using big data: Case study from new jersey, J. Transp. Saf. Secur. 11 (2019) 491–519, http://dx.doi.org/10.1080/19439962.2018.1436105.
[36] J. Chen, J. Liu, Q. Peng, Y. Yin, Strategies to enhance the resilience of an urban rail transit network, Transp. Res. Record (2021) http://dx.doi.org/10.1177/03611981211037888.
[37] X. Xu, A. Chen, Z. Zhou, S. Bekhor, Path-based algorithms to solve C-logit stochastic user equilibrium assignment problem, Transp. Res. Rec. 2279 (2012) 21–30, http://dx.doi.org/10.3141/2279-03.
[38] Y. Yin, J. Chen, M. Zhu, J. Liu, Repair strategies for failure of urban rail transit stations, J. Southwest Jiaotong Univ. 55 (2020) 869–876, http://dx.doi.org/10.3969/j.issn.0258-272420191133.
[39] J. Liu, P.M. Schonfeld, Q. Peng, Y. Yin, Measures of travel reliability on an urban rail transit network, J. Transp. Eng. Pt A-Syst. 146 (6) (2020) http://dx.doi.org/10.1061/JTEPBS.0000361.
[40] J. Liu, P.M. Schonfeld, A. Li, Q. Peng, Y. Yin, Effects of line-capacity reductions on urban rail transit system service performance, J. Transp. Eng. Pt A-Syst. 146 (10) (2020) http://dx.doi.org/10.1061/JTEPBS.0000445.
[41] A.M. Pnevmatikou, M.G. Karlaftis, K. Kepaptsoglou, Metro service disruptions: How do people choose to travel? Transportation 42 (2015) 933–949, http://dx.doi.org/10.1007/s11116-015-9656-4.
[42] Z. Lin, M. Jiang, J. Liu, B. Si, Improved logit model and method for urban rail transit network assignment, J. Transp. Syst. Eng. Inf. Technol. 12 (2012) 145–151, http://dx.doi.org/10.16097/j.cnki.1009-6744.2012.06.015.
[43] C. Malandri, A. Fonzone, O. Cats, Recovery time and propagation effects of passenger transport disruptions, Physica A 505 (2018) 7–17, http://dx.doi.org/10.1016/j.physa.2018.03.028.
[44] W. Li, R. Xu, Simulation of passenger travel behaviors on urban rail transit in emergency, J. East China Jiaotong Uni. 32 (2015) 46–53, http://dx.doi.org/10.16749/j.cnki.jecjtu.2015.02.006.
[45] H. Xu, L. Jiao, S. Chen, M. Deng, N. Shen, An innovative approach to determining high-risk nodes in a complex urban rail transit station: A perspective of promoting urban sustainability, Sustainability 10 (2018) 2456, http://dx.doi.org/10.3390/su10072456.
[46] C. Li, J. Huang, B. Wang, Y. Zhou, Y. Bai, Y. Chen, Spatial–temporal correlation prediction modeling of origin–destination passenger flow under urban rail transit emergency conditions, IEEE Access 7 (2019) 162353-162365, http://dx.doi.org/10.1109/ACCESS.2019.2951604.
[47] National People's Congress Standing Committee, Law of People's Republic of China on work safety, 2014.
[48] R. Tarjan, Depth-first search and linear graph algorithms, SIAM J. Comput. 1 (1972) 146–160, http://dx.doi.org/10.1109/SWAT.1971.10.
[49] R.W. Floyd, Algorithm 97: shortest path, Commun. ACM 5 (1962) 345, http://dx.doi.org/10.1145/367766.368168.
[50] H.X. Liu, X. He, B. He, Method of successive weighted averages (MSWA) and self-regulated averaging schemes for solving stochastic user equilibrium problem, Netw. Spat. Econ. 9 (2009) 485–503, http://dx.doi.org/10.1007/s11067-007-9023-x.
[51] https://lbs.amap.com/. (Accessed 6 October 2020).